Electronic Supplementary Material (ESI) for ChemComm.

ELECTRONIC SUPPORTING INFORMATION (ESI)

for

Counteranion-dependent mechanochromism of a photoluminescent platinum(II) complex with mixed terpyridine and thioglucose

Naoki Kitani, Naoto Kuwamura, Toshiaki Tsukuda, Nobuto Yoshinari and Takumi Konno*

Preparation of complexes.

[Pt(H$_4$tg-*S*)(terpy)]ClO$_4$ ([1]ClO$_4$). To an orange solution containing [PtCl(terpy)]Cl·2H$_2$O [1] (0.20 g, 0.37 mmol) in 40 mL of water was added a solid sample of KH$_4$tg·H$_2$O [2] (0.11 g, 0.41 mmol). The mixture was stirred at room temperature for 10 min, which gave a red solution. To the red solution was added a 1.0 M NaClO$_4$ aqueous solution (5 mL), followed by allowing it to stand at room temperature for 4 days. The resulting orange fiber crystals were collected by filtration. Yield: 0.25 g (87%). Anal. Calcd for [Pt(H$_4$tg)(terpy)]ClO$_4$·2H$_2$O ([**1**]ClO$_4$·2H$_2$O = $C_{21}H_{22}N_3ClO_9PtS$): C, 33.23; H, 3.45; N, 5.54%. Found: C, 33.29; H, 3.37; N, 5.58%. ^{1}H NMR (D$_2$O): δ 9.11 (2H, d, *J* = 5.6 Hz), 8.31 (1H, t, *J* = 8.2 Hz), 8.26 (2H, td, *J* = 7.8, 1.5 Hz), 8.13 (2H, d, *J* = 8.8 Hz), 8.09 (2H, d, *J* = 7.6 Hz), 7.71-7.68 (2H, m), 4.42 (1H, d, *J* = 8.8 Hz), 3.71 (1H, dd, *J* = 12.1, 1.3 Hz), 3.51 (1H, dd, *J* = 12.2, 5.4 Hz), 3.33-3.26 (4H, m). IR (cm^{-1}): 625, 1090 (ν(ClO$_4^-$)). Orange needle crystals suitable for X-ray analysis were obtained by the recrystallization of the fiber crystals from hot water.

[Pt(H$_4$tg-*S*)(terpy)]PF$_6$ ([1]PF$_6$). This complex-salt was obtained as orange fiber crystals by a method similar to that for [**1**]ClO$_4$, using a 1.0 M NH$_4$PF$_6$ aqueous solution instead of a 1.0 M NaClO$_4$ aqueous solution. Yield: 0.25 g (85%). Anal. Calcd for [Pt(H$_4$tg)(terpy)]PF$_6$·1.5H$_2$O ([**1**]PF$_6$·1.5H$_2$O = $C_{21}H_{25}F_6N_3O_{6.5}PPtS$) : C, 31.71; H, 3.17; N, 5.28%. Found: C, 31.57; H, 3.12; N, 5.34%. IR (cm^{-1}): 560, 842 (ν(PF$_6^-$)). Orange needle crystals suitable for X-ray analysis were obtained by allowing the remaining filtrate to stand at room temperature.

Measurements.

The electronic absorption spectra were recorded with a JASCO V-660 spectrophotometer at room temperature. The IR spectra were recorded on a JASCO FT/IR-4100 infrared spectrometer using KBr disks at room temperature. The luminescent spectra were recorded on a JASCO FP-6600 spectrometer in solid state at room temperature. The light shorter than 370 nm was removed by using a glass filter. The emission spectra in the solid state were recorded by scanning 10 times with a rate

of 500 nm /min. The solid state emission spectrum was accumulated for 10 times scan The internal quantum yields were measured by the absolute method using a spectrofluorometer (Jasco FP-8500) with a fluorescence integrating sphere unit (Jasco ILFC-847) at an excitation wavelength of 340 nm using a Xe lamp as the light source, and the data were corrected using both deuterium and halogen lamps. The elemental analyses (C, H, N) were performed with Yanaco CHN Corder MT-5. The ^{1}H NMR spectra were recorded with a JEOL GSX400 spectrometer in D_2O. Sodium 4,4'-dimethyl-4-silapentane-1-sulfonate (DSS) was used as the internal standard. The molar conductivities were measured with a HORIBA DS12 conductivity meter. The powder X-ray diffraction measurement experiments were performed on a Bruker D2 PHASER.

X-ray crystallography.

Single-crystal X-ray diffraction measurements for [**1**]ClO_4 were performed on a Rigaku RAXIS RAPID imaging plate and Vari-Max with graphite monochromated Mo-Kα radiation (λ = 0.71075 Å) at 200 K. The measurements for [**1**]PF_6 were performed on a Rigaku R-AXIS VII imaging plate and Vari-Max with graphite monochromated Mo-Kα radiation (λ = 0.71075 Å) at 200 K. The intensity data were collected by the ω-scan technique and empirically corrected for absorption. The structures of the complexes were solved by direct methods using SHELXS97.[3] The structure refinements were carried out using full matrix least-squares (SHELXL-97).[3] Because of the quite thin needle-like shape of [**1**]ClO_4 (0.25 x 0.03 x 0.01 mm^3) and [**1**]PF_6 (0.15 x 0.01 x 0.01 mm^3), the X-ray absorption corrections were not effectively made. Thus, only heavy atoms were refined anisotropically (Pt, S, Cl, and O for [**1**]ClO_4 and Pt, S, and P for [**1**]PF_6), and others were refined by using isotropic models. Hydrogen atoms were placed at calculated positions. All structural parameters are summarized in the Tables S2-S4.

Computational details.

The electronic structures were calculated by using Gaussian09 software.[4] The density functional theory (DFT) and the time-dependent DFT (TD-DFT) calculations were performed by using the B3LYP function with Lanl2dz basis sets on Pt atom, 6-31G* basis sets on N, S atoms, and 6-31G basis sets on C, H, O atoms.[5] All of the geometries were taken directly from the single-crystal structure coordinates; a single-point calculation was performed on each asymmetric unit.

References.

1. (*a*) S. E. Hobert, J. T. Carney and S. D. Cummings, *Inorganica Chimica Acta*, 2001, **318**, 89; (*b*) J. X. McDermott, J. F. White and G. M. Whitesides, *J. Am. Chem. Soc.* 1976, **98**, 6521; (*c*) D. P. Gamblin, P. Garnier, S. Kasteren, N. J. Oldham, A. J. Fairbanks and B. G. Davis, *Angew. Chem. Int. Ed.* 2004, **43**, 828; (*d*) J. Ella-Menye, X. Nie and G. Wang, *Carbohydrate Research*, 2008, **343**, 1743; (*e*) G. J. L. Bernardes, E. J. Grayson, S. Thompson, J. M. Chalker, J. C. Errey, F. E. Oualid, T. D. W. Claridge and B. G. Davis, *Angew. Chem. Int. Ed.* 2008, **47**, 2244.

2. N. Yoshinari, N. Kitani and T. Konno, *Acta Crystallogr.* 2012, **C68**, m363.

3. Sheldrick, G. M. *Acta Crystallogr.* 2008, **A64**, 112.

4. Gaussian 09, Revision ***A.1***, M. J. Frisch, G. W. Trucks, H. B. Schlegel, G. E. Scuseria, M. A. Robb, J. R. Cheeseman, G. Scalmani, V. Barone, B. Mennucci, G. A. Petersson, H. Nakatsuji, M. Caricato, X. Li, H. P. Hratchian, A. F. Izmaylov, J. Bloino, G. Zheng, J. L. Sonnenberg, M. Hada, M. Ehara, K. Toyota, R. Fukuda, J. Hasegawa, M. Ishida, T. Nakajima, Y. Honda, O. Kitao, H. Nakai, T. Vreven, J. A. Montgomery, Jr., J. E. Peralta, F. Ogliaro, M. Bearpark, J. J. Heyd, E. Brothers, K. N. Kudin, V. N. Staroverov, R. Kobayashi, J. Normand, K. Raghavachari, A. Rendell, J. C. Burant, S. S. Iyengar, J. Tomasi, M. Cossi, N. Rega, J. M. Millam, M. Klene, J. E. Knox, J. B. Cross, V. Bakken, C. Adamo, J. Jaramillo, R. Gomperts, R. E. Stratmann, O. Yazyev, A. J. Austin, R. Cammi, C. Pomelli, J. W. Ochterski, R. L. Martin, K. Morokuma, V. G. Zakrzewski, G. A. Voth, P. Salvador, J. J. Dannenberg, S. Dapprich, A. D. Daniels, O. Farkas, J. B. Foresman, J. V. Ortiz, J. Cioslowski and D. J. Fox, Gaussian, Inc., Wallingford CT, 2009.

5. (*a*) A. D. Becke, *Phys. Rev. A* 1988, **38**, 3098; (*b*) A. D. Becke, *J. Chem. Phys.* 1993, **98**, 5648; (*c*) C. Lee, W. Yang and R. G. Parr, *Phys. Rev. B* 1988, **37**, 785.

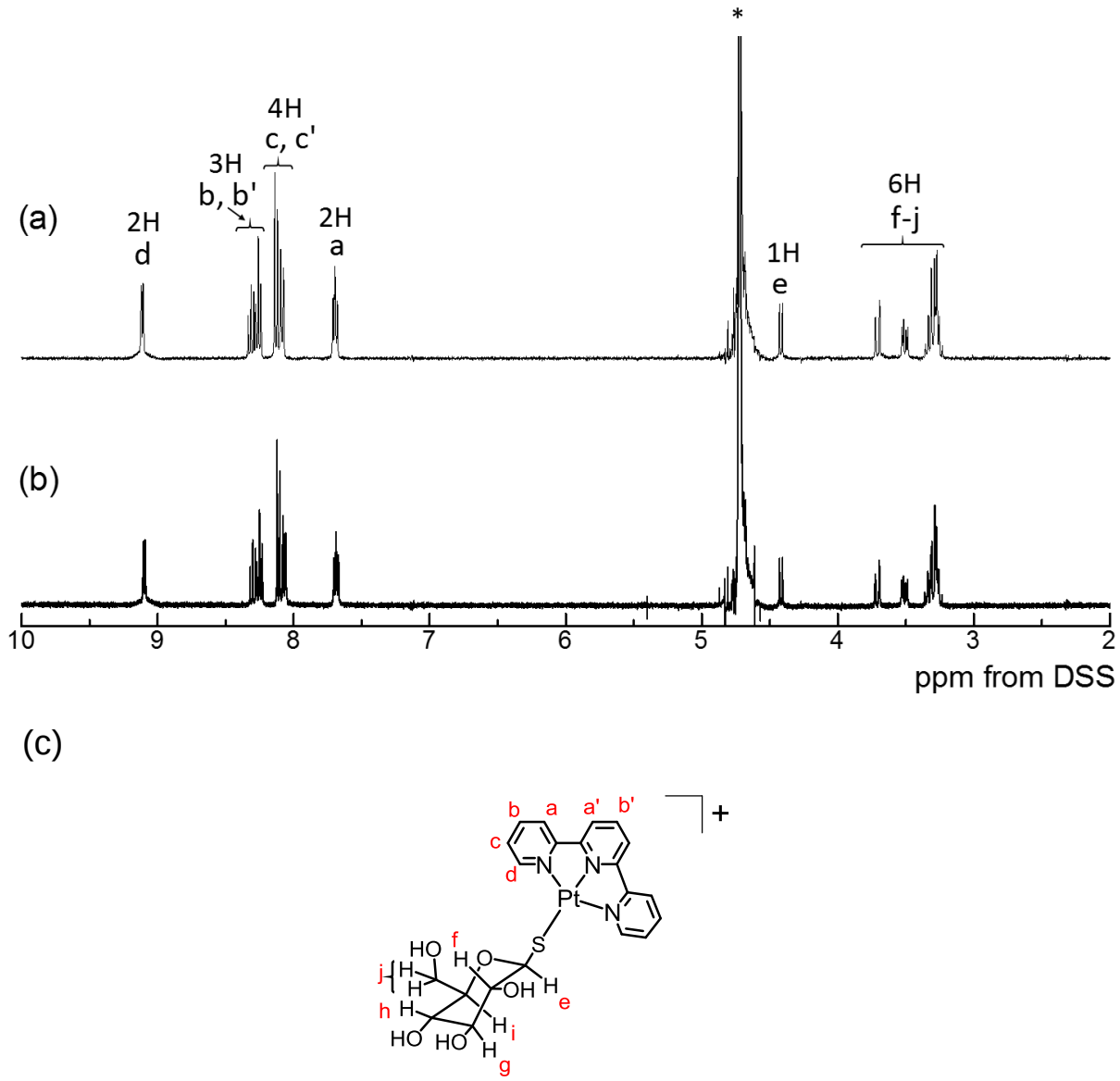

(c)

Fig. S1. ^{1}H NMR spectra of (a) [**1**]ClO_4 and (b) [**1**]PF_6 in D_2O. (*) indicates the signal from H_2O. (c) Drawing of the structure of [**1**]$^{+}$.

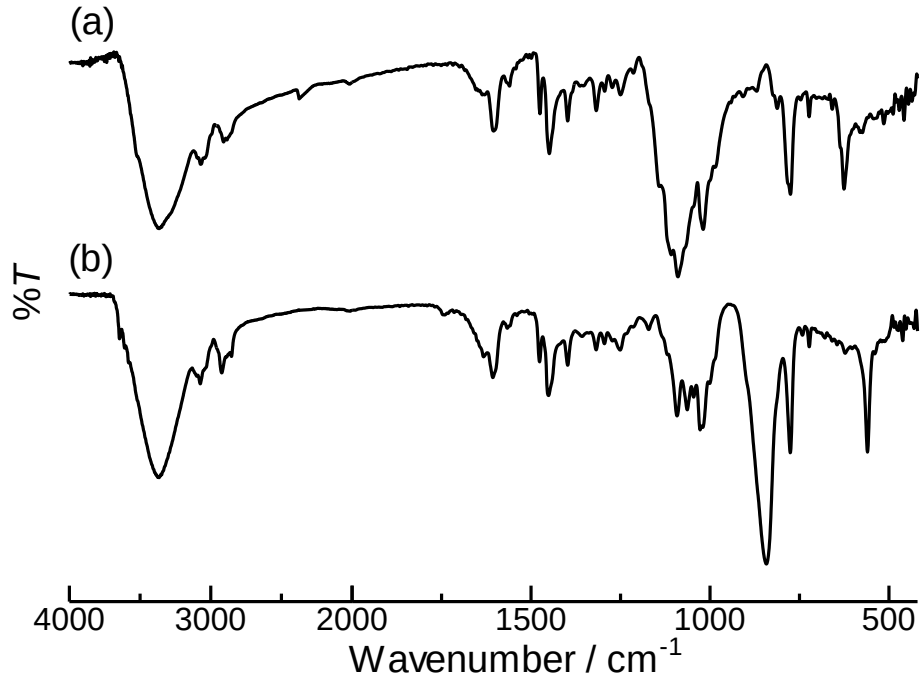

Fig. S2. IR spectra of (a) [**1**]ClO_4 and (b) [**1**]PF_6.

(a)

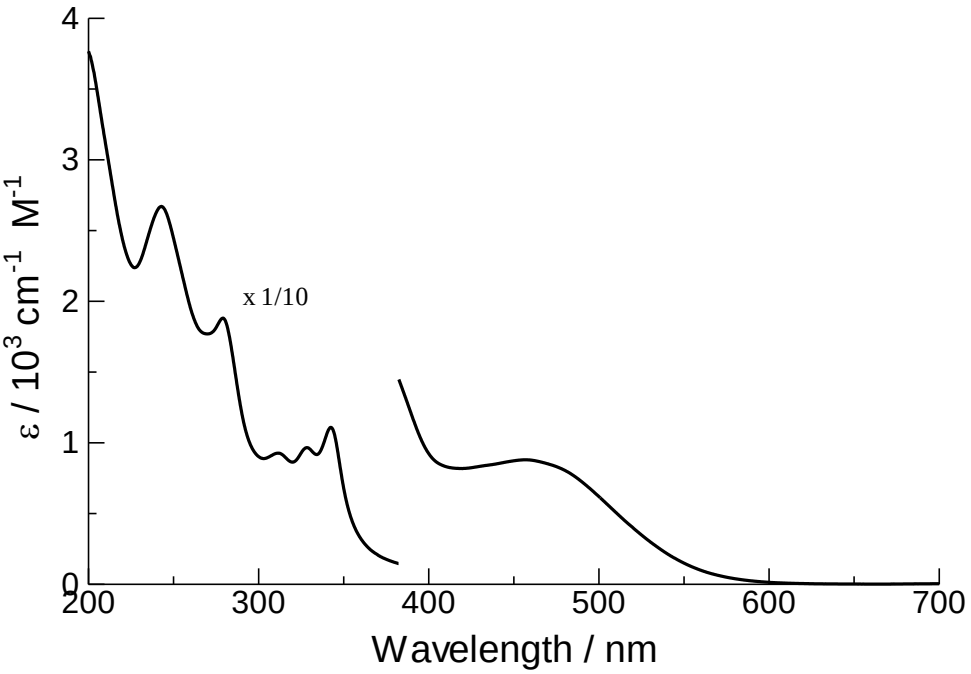

(b)

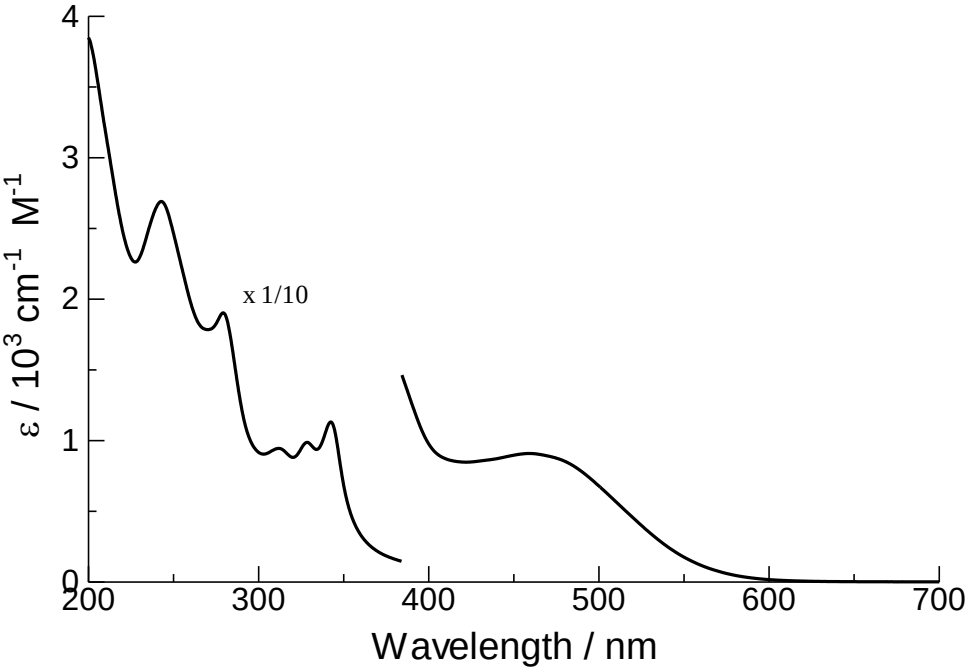

Fig. S3. Electronic absorption spectrum of (a) [**1**]ClO_4 and (b) [**1**]PF_6 in H_2O.

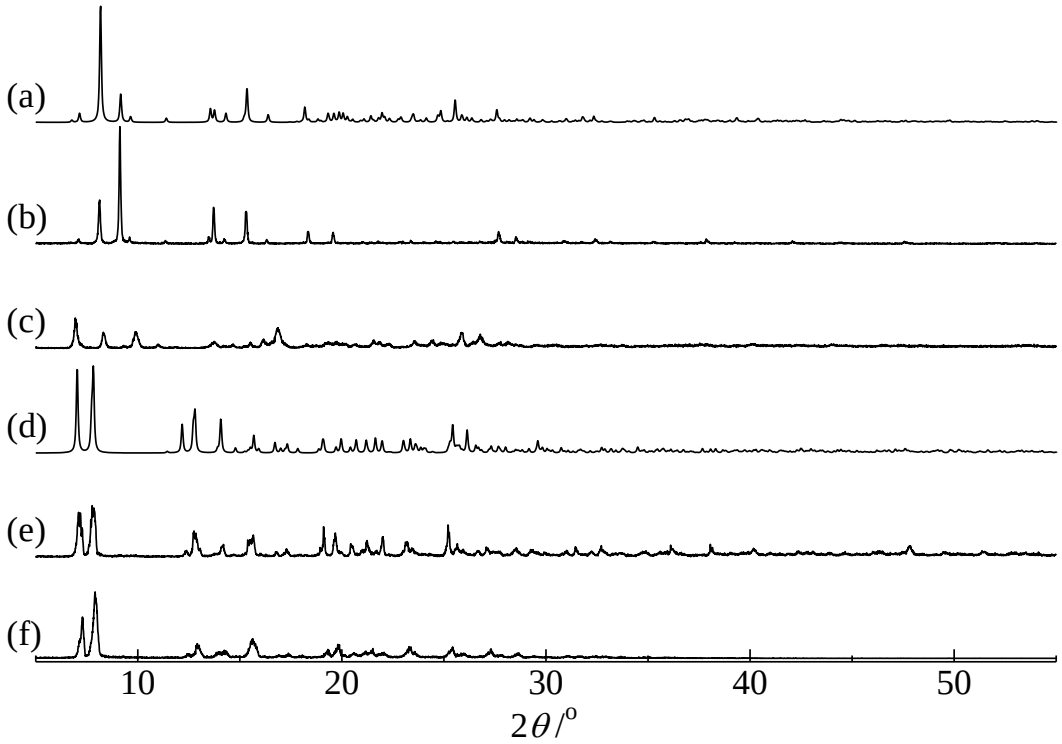

Fig. S4. Powder X-ray diffraction spectra of [**1**]ClO_4 (a) simulated based on the single-crystal X-ray analytical data, (b) before grinding and (c) after grinding. Powder X-ray diffraction spectra of [**1**]PF_6 (d) simulated based on the single-crystal X-ray analytical data, (e) before grinding and (f) after grinding.

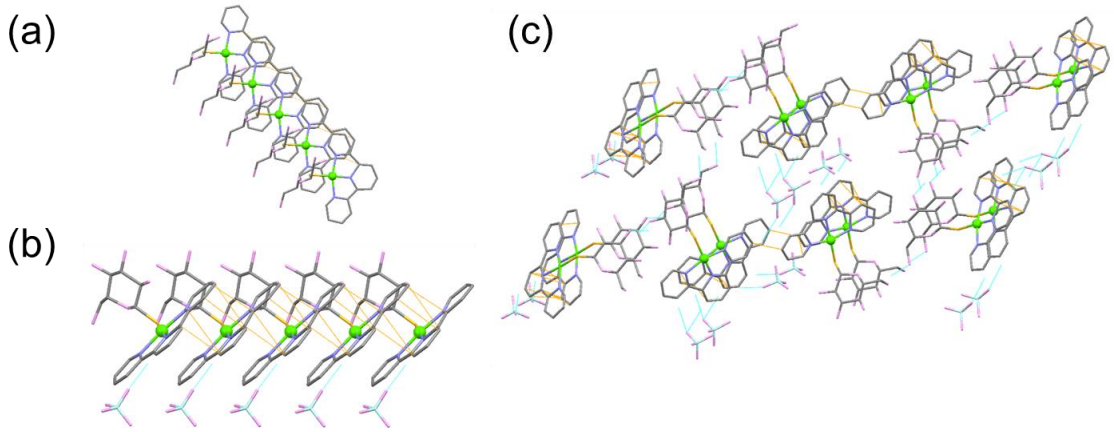

Fig. S5. (a) Top and (b) side views of the 1D chain structure and (c) the 3D packing structure in [**1**]$ClO_4 \cdot 2H_2O$. Orange and blue dotted lines indicate the π–π and hydrogen bonding interactions, respectively. H atoms are omitted for clarity. Pt: light green, S: yellow, Cl: pale blue, O: pink N: blue, C: gray.

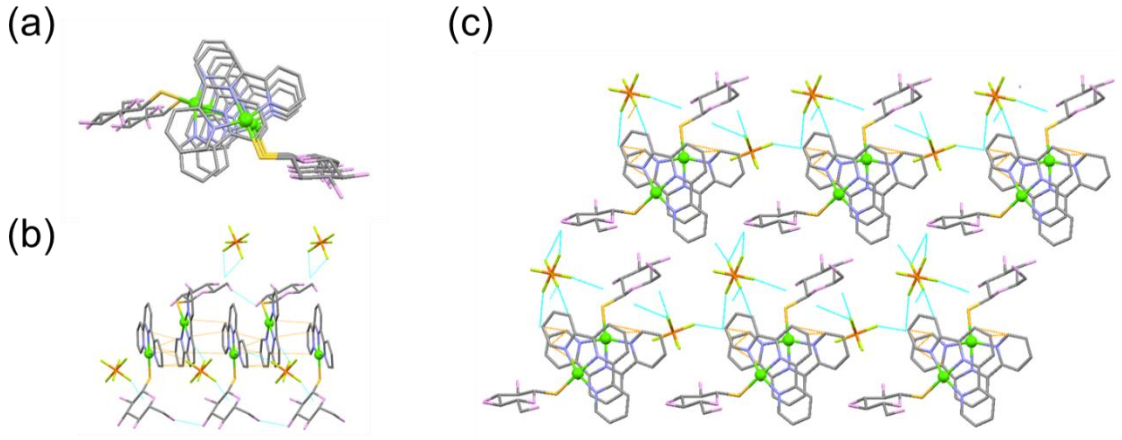

Fig. S6. (a) Top and (b) side views of the 1D chain structure and (c) the 3D packing structure in [**1**]$PF_6 \cdot 1.5H_2O$. Orange and blue dotted lines indicate the π–π and hydrogen bonding interactions, respectively. H atoms are omitted for clarity. Pt: light green, S: yellow, P: orange, F: olive green, O: pink N: blue, C: gray.

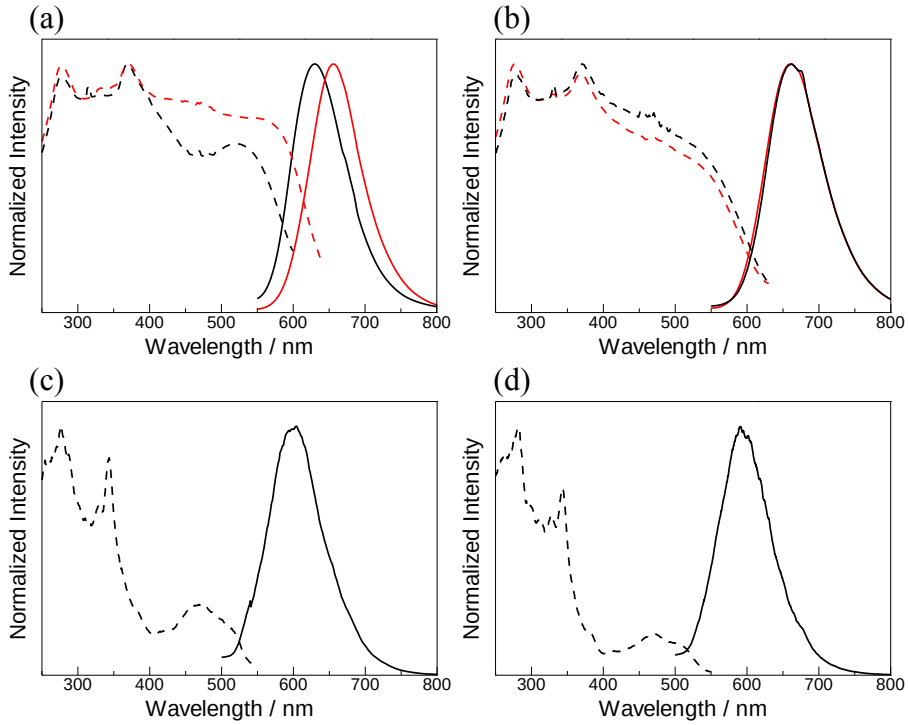

Fig. S7. Emission and excitation spectra of (a) [**1**]ClO_4 and (b) [**1**]PF_6 in the solid state at room temperature before grinding (black line) and after grinding (red line). Emission and excitation spectra of (c) [**1**]ClO_4 and (d) [**1**]PF_6 in H_2O/EtOH at 77 K. Excitation wavelength is 340 nm.

[Pt(H_4tg-*S*)(terpy)]ClO_4

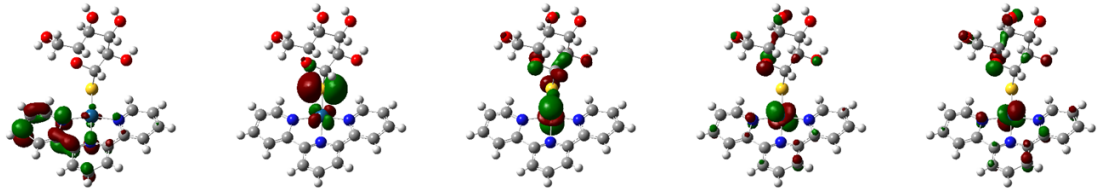

LUMO (terpy(44%)) | HOMO (Pt(14%), S(75%)) | HOMO-1 (Pt(54%), S(12%)) | HOMO-2 (Pt(39%)) | HOMO-3 (Pt(30%))

[Pt(H_4tg-*S*)(terpy)]PF_6

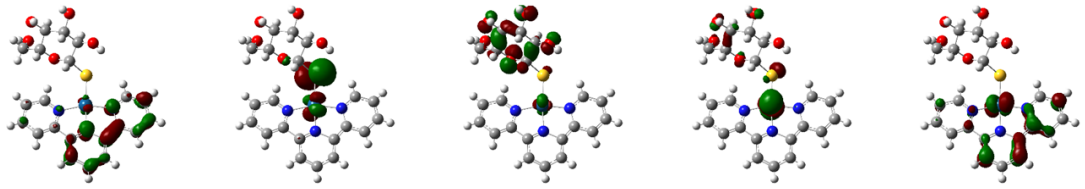

LUMO (terpy(23%)) | HOMO (Pt(20%), S(66%)) | HOMO-1 (H_4tg(36%)) | HOMO-2 (Pt(62%)) | HOMO-3 (Pt(30%), terpy(20%))

Fig. S8. The contour plots of molecular orbitals of the complex cations in [**1**]ClO_4 and [**1**]PF_6. The surfaces are drawn at 0.05 a.u. level.

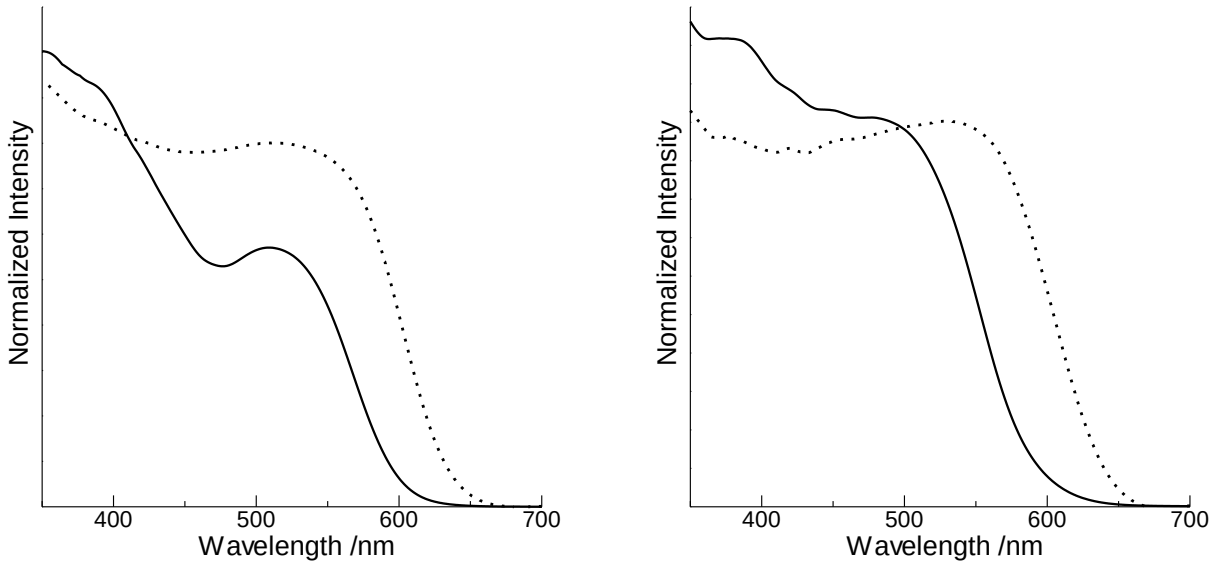

Fig. S9. Diffuse reflection spectra of [**1**]ClO_4 (left) and [**1**]PF_6 (right) in the solid state before grinding (solid line) and after grinding (dashed line).

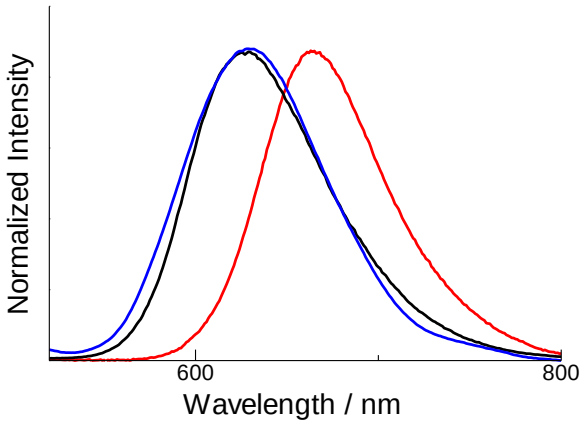

Fig. S10. Emission spectra of [**1**]ClO_4 in the solid state before grinding (black line), after grinding (red line), and after recrystallization (blue line). Excitation wavelength is 340 nm.

Table S1. Electronic absorption spectral data of [**1**]ClO_4 in water.

λ_{max} / nm (ε / 10^3 cm^{-1} M^{-1})
456.6 (0.8802)
341.8 (11.06)
328.2 (9.663)
311.0 (9.267)
279.0 (18.81)
242.4 (26.69)

Table S2. Crystallographic data of complexes.

	[**1**]$ClO_4 \cdot 2H_2O$	[**1**]$PF_6 \cdot 1.5H_2O$
Chemical formula	$C_{21}H_{26}ClN_3O_{11}PtS$	$C_{21}H_{25}F_6N_3O_{6.5}PPtS$
Formula weight (*M*)	759.05	795.56
Crystal system	Monoclinic	Triclinic
Space group	$P2_1$	$P1$
a / Å	4.9262(11)	7.9715(3)
b / Å	38.578(9)	13.0562(4)
c / Å	13.082(4)	14.1600(5)
α /°	90	63.162(5)
β /°	94.038(8)	89.461(7)
γ /°	90	77.050(6)
V / Å^3	2479.9(10)	1274.4(1)
Z	4	2
T / K	200(2)	200(2)
R(int)	0.1765	0.0593
D_{calcd} / g cm^{-3}	2.033	2.073
μ (Mo Kα), mm^{-1}	51.97	57.184
θ_{Max} /°	27.48	27.50
Miller index ranges	$-6 \le h \le 6$	$-10 \le h \le 10$
	$-49 \le k \le 49$	$-16 \le k \le 16$
	$-16 \le l \le 16$	$-17 \le l \le 18$
Reflections collected	22898	14747
Refinement method	Full-matrix least-square on F^2	Full-matrix least-square on F^2
Data / restraints / Parameters	11010 / 7 / 447	9887 / 3 / 349
Flack	0.0018(16)	0.003(13)
R_1 ($I>2\sigma(I)$)[a]	0.1332	0.0748
wR_2[b]	0.2876	0.1897
Goodness-of-fit on F^2	1.123	1.140
Treatment of hydrogen atoms	constr	constr
CCDC number	1005469	1005470

[a] $R_1 = \Sigma|(|Fo|-|Fc|)| / \Sigma(|Fo|)$. [b] $wR_2 = [\Sigma w(Fo^2-Fc^2)^2 / \Sigma w(Fo^2)^2]^{1/2}$.

Table S3. Selected bond distances and angles of [**1**]$ClO_4 \cdot 2H_2O$.

Bond distances (Å)			
Pt(1)-N(1)	2.11(3)	Pt(2)-N(4)	1.97(2)
Pt(1)-N(2)	1.89(2)	Pt(2)-N(5)	2.08(3)
Pt(1)-N(3)	2.08(3)	Pt(2)-N(6)	2.03(3)
Pt(1)-S(1)	2.326(7)	Pt(2)-S(2)	2.304(9)
Bond angles (˚)			
N(1)-Pt(1)-N(2)	84.2(10)	N(4)-Pt(2)-N(5)	79.6(11)
N(1)-Pt(1)-N(3)	163.4(10)	N(4)-Pt(2)-N(6)	161.3(11)
N(2)-Pt(1)-N(3)	79.2(10)	N(5)-Pt(2)-N(6)	81.8(11)
N(1)-Pt(1)-S(1)	97.5(7)	N(4)-Pt(2)-S(2)	101.5(8)
N(2)-Pt(1)-S(1)	178.0(7)	N(5)-Pt(2)-S(2)	173.6(7)
N(3)-Pt(1)-S(1)	99.0(8)	N(6)-Pt(2)-S(2)	97.1(9)
C(1)-S(1)-Pt(1)	103.1(9)	C(22)-S(2)-Pt(2)	102.3(10)

Table S4. Selected bond distances and angles of [**1**]$PF_6 \cdot 1.5H_2O$.

Bond distances (Å)			
Pt(1)-N(1)	1.998(14)	Pt(2)-N(4)	2.013(19)
Pt(1)-N(2)	1.98(3)	Pt(2)-N(5)	1.986(16)
Pt(1)-N(3)	2.032(14)	Pt(2)-N(6)	2.017(16)
Pt(1)-S(1)	2.294(7)	Pt(2)-S(2)	2.281(4)
Bond angles (˚)			
N(1)-Pt(1)- N(2)	81.3(7)	N(4)-Pt(2)-N(5)	82.9(7)
N(1)-Pt(1)- N(3)	163.3(8)	N(4)-Pt(2)-N(6)	161.7(6)
N(2)-Pt(1)-N(3)	81.9(8)	N(5)-Pt(2)-N(6)	78.9(7)
N(1)-Pt(1)-S(1)	96.9(6)	N(4)-Pt(2)-S(2)	93.5(4)
N(2)-Pt(1)-S(1)	176.2(5)	N(5)-Pt(2)-S(2)	176.2(6)
N(3)-Pt(1)-S(1)	99.8(6)	N(6)-Pt(2)-S(2)	104.6(5)
C(1)-S(1)-Pt(1)	108.1(7)	C(22)-S(2)-Pt(2)	112.5(5)

Table S5. Energy, oscillator strength and major contribution of calculated transitions for [**1**]ClO_4 and [**1**]PF_6.

Excited state	Energy / eV (/ nm)	Oscillator strength	Major contributions
[**1**]ClO_4			
1	2.2226 (557.84)	0.0027	HOMO –> LUMO (99%)
2	2.7688 (447.79)	0.0009	HOMO –> LUMO+1 (99%)
3	3.0456 (407.10)	0.0034	HOMO-1 –> LUMO (80%)
			HOMO-2 –> LUMO (13%)
4	3.3131 (374.23)	0.0103	HOMO-2 –> LUMO (55%)
			HOMO-3 –> LUMO (30%)
[**1**]PF_6			
1	2.3866 (519.51)	0.0547	HOMO –> LUMO (99%)
2	2.8682 (432.28)	0.0251	HOMO –> LUMO+1 (99%)
3	3.0892 (401.35)	0.0033	HOMO-1 –> LUMO (31%)
			HOMO-2 –> LUMO (58%)
4	3.3060 (375.03)	0.0170	HOMO-3 –> LUMO (81%)